Table 1 Primer and probe sequences

Primer or probe	Sequence (5′-3′)	Target
first-*Alu*-F	AGCCTCCCGAGTAGCTGGGA	Integrated HIV-1 DNA (first-round PCR)
first-*Alu*-R	TTACAGGCATGAGCCACCG	
first-gag-R	CAATATCATACGCCGAGAGTGCGCGCTTCAGCAAG	
second-LTR-F	TTGTTACACCCTATGAGCCAGC	Integrated HIV-1 DNA (second-round PCR)
second-tag-R	CAATATCATACGCCGAGAGTGC	
probe-1	AGTGTGTGCCCGTCTGTTGTGTGACTC*	
probe-2	CGCTTCAGCAAGCCGAGTCCTGC*	
total-F	CCGTCTGTTGTGTGACTCTGG	Total HIV-1 DNA
total-R	GAGTCCTGCGTCGAGAGATCT	
total-probe	TCTAGCAGTGGCGCCCGAACAGG*	
circle-F	CCCTCAGACCCTTTTAGTCAGTG	2LTR circle DNA
circle-R	TGGTGTGTAGTTCTGCCAATCA	
circle-probe	TGTGGATCTACCACACACAAGGCTACTTCC*	

*Modified with FAM at the 5′ end and with TAMRA at the 3′ end. The tag sequence in the first-gag-R primer is underlined

Alu-targeting primers that annealed to conserved regions of the *Alu* repeat element (Fig. 1a). Since *Alu* elements are present in either orientation relative to the integrated provirus, the use of two outward-facing *Alu* primers optimized the amplification of *Alu*-gag sequences integrated into the host cell genome (Fig. 1a). To decrease amplification of nonintegrated reverse transcription products, we used an HIV-1 gag-specific primer extended with an artificial tag sequence at the 5′ end of the oligonucleotide (first-gag-R) in the first round of amplification and the primer which matches this artificial sequence (second-tag-R) in the second-round PCR (Fig. 1b).

The method 1 shown in Fig. 1b is equivalent to previously established real-time nested PCR assay and the method 2 is a novel assay developed by us. In the second-round PCR using the tag-specific primer and the LTR primer, the first-round PCR product could be amplified with lower background by the method 1. However, unintegrated viral DNA could be amplified in the method 1 even when the tag-specific primer was used for amplification. Because one twenty fifth of the reaction mixture after 12 cycles of the first-round PCR was used as a template for the second-round PCR, unintegrated reverse transcription products could be amplified with the forward primer for second-round PCR (second-LTR-F) and the residual reverse primer for first-round PCR (first-gag-R) (Fig. 1b). To prevent non-specific amplification of unintegrated reverse transcription products, we designed a new method (method 2) using probe-2 which has a sequence overlapping the first-gag-R primer. Probe-2 can preferentially hybridize to the target sequence and inhibit hybridization of the residual first-gag-R primer during the second-round PCR, because the melting temperature of probe-2 is much higher than that of the first-gag-R primer (Fig. 1b).

Specificity of the novel real-time nested PCR assay.

To assess the extent of non-specific amplification of unintegrated reverse transcription products in method 1 and method 2, we compared the fluorescence curves generated during the second-round PCR after three different first-round reactions: (1) in the presence of 3 primers (first-*alu*-F, first-*alu*-R, first-gag-R) with polymerase (primer+ / polymerase+), (2) in the presence of 3 primers without polymerase (primer+/polymerase−), and (3) in the absence of 3 primers without polymerase (primer−/ polymerase−). The fluorescence curve of primer+/polymerase+in the method 1 significantly shifted to the left in comparison to that of the primer−/polymerase−reaction (Fig. 2a). However, the fluorescence curve of primer+/polymerase−in the method 1 shifted as much as that of primer+/polymerase+ (Fig. 2a). This means that the extent of amplification of unintegrated reverse transcription products with the second-LTR-F primer and the first-gag-R primer was considerable. Probe-2, which was used in the method 2, preferentially hybridized to the target sequence and inhibited hybridization of the first-gag-R primer during the second-round PCR, because the melting temperature of probe-2 is much higher than that of the first-gag-R primer (Fig. 1b). As shown in Figure 2b, the fluorescence curve of primer+/ polymerase− in the method 2 shifted to the right dramatically compared with the curve of primer+/polymerise-in the method 1. The shift by using probe-2 instead of probe-1 was about 4 log10 units (17 cycles), which indicated that the specificity of the method 2 was much higher than that of the method 1.

Sensitivity of the novel real-time nested PCR assay.

The copy number of integrated HIV-1 DNA was determined in reference to a standard curve given by an array of serially

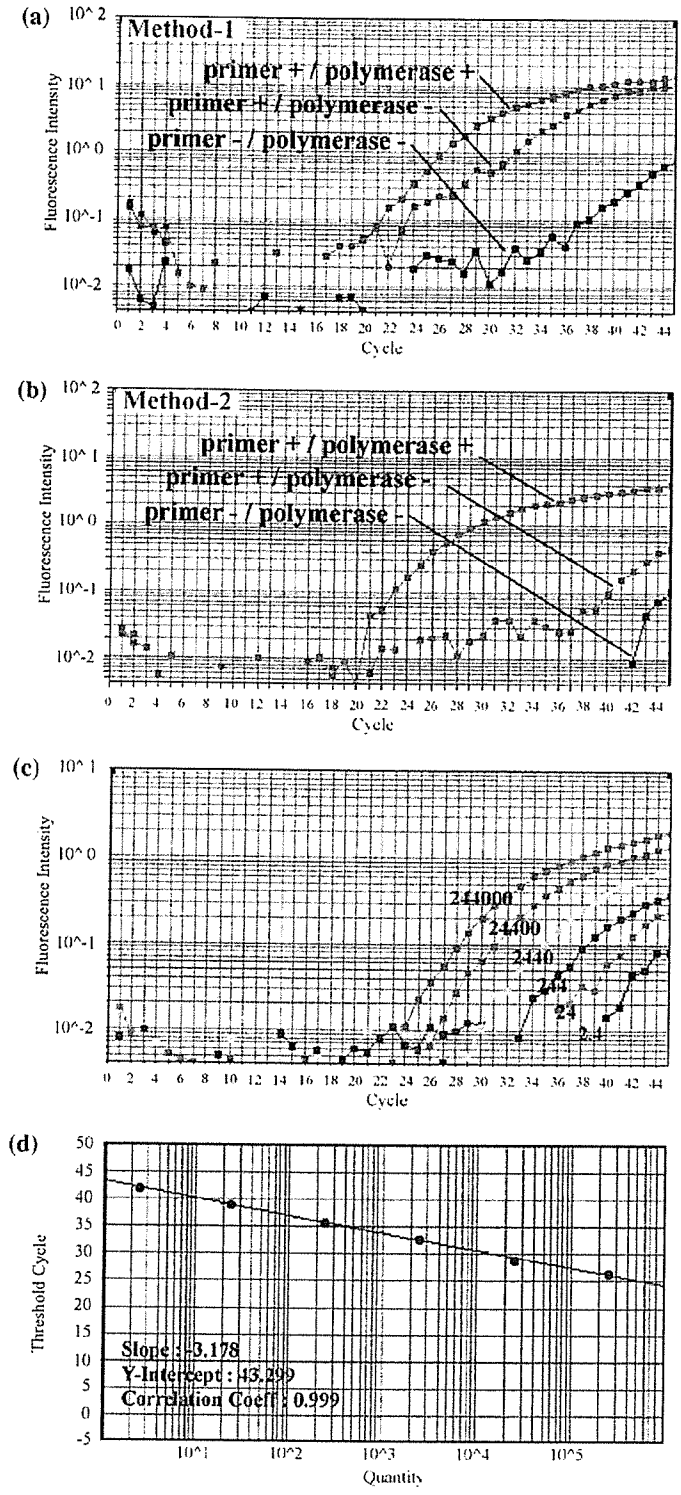

Fig. 2 Characteristics of real-time nested PCR. (**a** and **b**) Fluorescence curves generated by amplification of provirus DNA from HL60 cells infected with VSV-G-pseudotyped NLE delta env virus. (**a**) Fluorescence curves of probe-1 used in method 1. (**b**) Fluorescence Curves of probe-2 used in method 2. (**c**) Fluorescence curves generated by two-step amplification of serial dilutions of Jurkat/NL-bsr cell DNA. The copy numbers for each standard DNA are shown on the corresponding fluorescence curve. (**d**) Linear regression to quantify integrated HIV-1 DNA

diluted Jurkat/NL-bsr cell DNA mixed with uninfected Jurkat cell DNA to yield 100,000 cell equivalents. In our system, the regression obtained from amplification of serial dilutions of the integrated HIV-1 DNA was linear over a 6-log 10-unit range, and this *Alu*-HIV nested PCR allowed the detection of approximately three proviruses in 100,000 cell equivalents (Fig. 2c and 2d). The sensitivity of our system is as high as that of previously reported methods [15–18].

Analysis of early HIV-1 DNA synthesis in Jurkat cells infected with VSV-G-pseudotyped virus

To assess the time point when integration of HIV-1 takes place, we quantified integrated HIV-1 DNA in a single round of viral replication with the novel real-time nested PCR assay.

Total HIV-1 DNA was detected 3 h post infection and reached a maximum of 7,726 copies per 1000 cells at 5 h post infection (Fig. 3a). Subsequently a steep decrease phase and a slow decrease phase were observed. This novel real-time nested PCR assay detected integrated HIV-1 DNA within 3 h of infection, which indicated that reverse transcription products were imported to the nucleus immediately and integrated into the host cell genome very rapidly (Fig. 3b). The copy number of integrated proviruses reached a maximum of 1398 copies per 1000 cells at 5 h post infection and remained at the same level after this time point, which suggested that HIV-1 integration was completed by 5 h post infection in Jurkat cells (Fig. 3b). Two-LTR circles were detected by 3 h post infection but the copy number of 2LTR circles was not as high as that of integrated HIV-1 DNA. (Fig. 3c).

Comparison of viral DNA synthesis in Jurkat cells, U937 cells, resting PBMCs and activated PBMCs

We compared the kinetics of viral DNA synthesis in several kinds of cells to elucidate the relationship between viral DNA synthesis and status of cells (Fig. 4). Jurkat cells, U937 cells, unstimulated PBMCs and PHA/IL-2-activated PBMCs were infected with VSV-G pseudotyped HIV-1 and these cells were lysed with DNA extraction buffer at 3 h, 6 h, 12 h, 24 h and 48 h post infection. Time points of sample collection were determined based on the result of detailed kinetic analysis in Jurkat cells (Fig. 3).

Efficiency of reverse transcription was quite different in each type of cells. Jurkat cells and U937 cells were highly active in reverse transcription (Fig. 4a) and activated PBMCs were moderately active (Fig. 4b). In resting PBMCs reverse transcription efficiency was very low (Fig. 4b). Two cell lines with higher reverse transcription activity, Jurkat cells and U937 cells, exhibited three phases in the kinetics of total DNA: a rapid rising phase, a steep falling phase and a slow falling phase (Fig. 4a). Activated and resting PBMCs, which showed lower reverse transcription efficiency, exhibited only a slow rising phase (Fig. 4b).

The kinetics of viral DNA integration was also dependent on the cells. Integration of viral DNA in Jurkat cells and U937 cells was completed by 12 h post infection (Fig. 4c, d). Activated PBMCs showed complete integration in 24 h (Fig. 4d). The cope number of proviral DNA in resting PBMCs reached a maximum level at 48 h (Fig. 4d). Efficiency of 2LTR circle formation was different in each cell type. Synthesis of two LTR circles reached its peak at the same time point when viral DNA integration reached its maximum level (Fig. 4e, f). Ratio of 2LTR DNA to proviral DNA was low in all cells (0.1–0.6%)

Discussion

We could have developed a novel assay with high specificity and sensitivity to quantify integrated viral DNA of HIV-1. Our study showed that specificity of this nested PCR assay is much higher than that of the previously reported methods [15–19].

We could find four previous methods to quantify integrated viral DNA: (1) methods based on one-step amplification, (2) methods based on nested PCR using linker-primer (nested LP-PCR), (3) methods based on real-time nested PCR using *Alu*-specific primers and a virus-specific primer without tag sequence, (4) methods based on real-time nested PCR using *Alu*-specific primers and a virus-specific primer with tag sequence.

The novel real-time nested PCR assay detected integrated HIV-1 DNA as early as 3 h after infection while the one-step amplification method allowed the detection of proviral DNA later than 12 h [20] or 24 h [19] after infection. The delayed detection of integrated HIV-1 DNA in the one-step real-time PCR might be due to the limited sensitivity of this assay.

Other methods based on nested LP-PCR had been devised [15, 16]. The protocol of the nested LP-PCR involved many experimental steps, one of which is amplification of LTR in the second-round PCR. The nested LP-PCR amplified the LTR sequence and did not prevent the amplification of unintegrated forms of HIV-1 because of the absence of a tag sequence in the primer.

Recently, a real time nested PCR method with the *Alu* element-specific primers and HIV-1 gag-specific primer without tag sequence was described, in which the LTR sequence was amplified during the second-round PCR [17]. This real-time nested PCR did not prevent the amplification of unintegrated forms of HIV-1 due to the lack of tag sequence in the primer.

More recently, Brussel et al. [18] developed a new real-time nested PCR using an extended LTR primer with a tag sequence for the first-round PCR and the tag-specific primer for the second-round PCR to amplify only products from the first-round PCR. However, even this well-devised method could not prevent the residual tagged primer used in first-round PCR from annealing to the unintegrated forms of HIV-1 DNA, which resulted in lower specificity

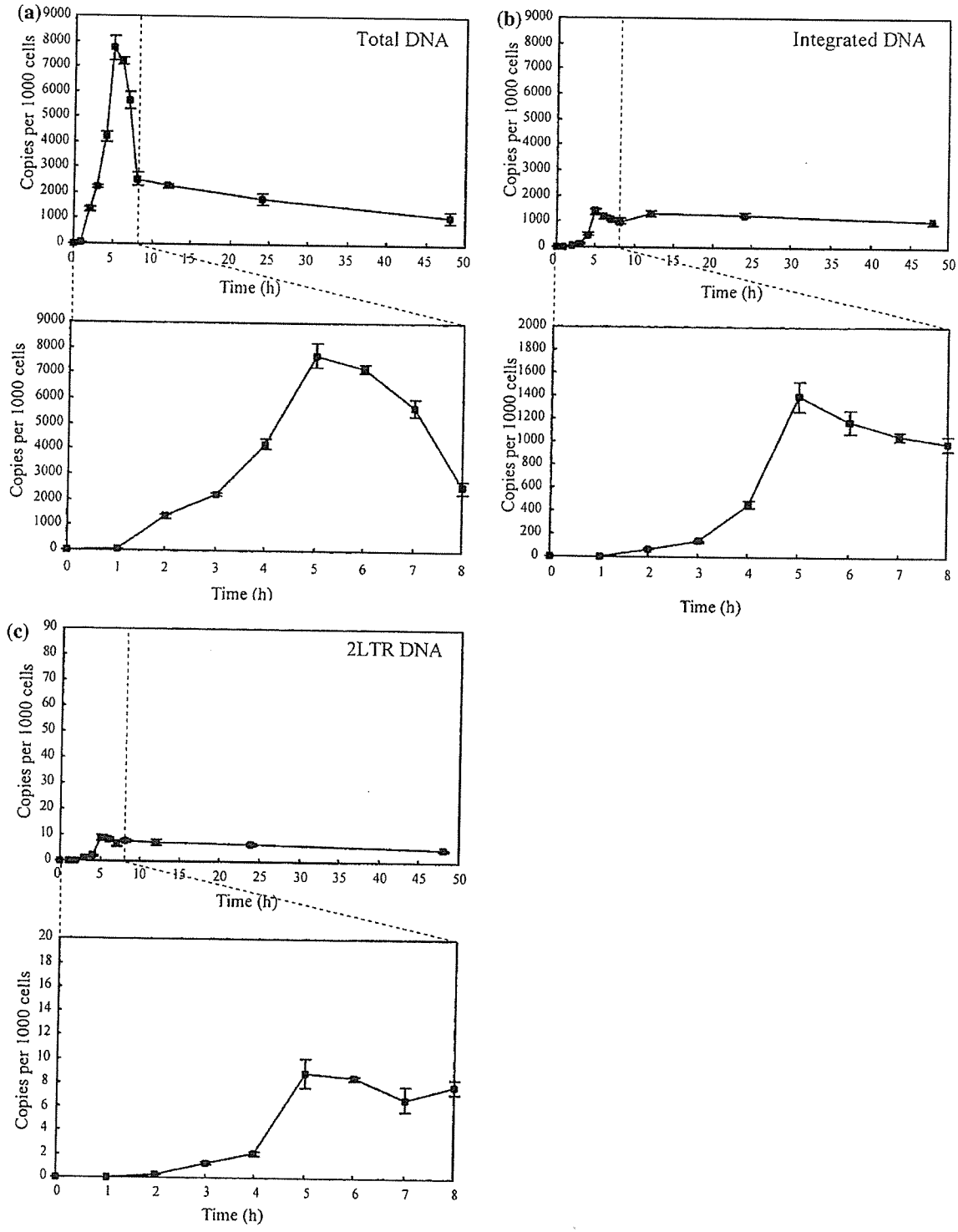

Fig. 3 Detailed quantification of HIV-1 DNA during a single round infection of Jurkat cells with VSV-G-pseudotyped NL-E delta env virus. (**a**) Time course analysis of total HIV-1 DNA, (**b**) integrated HIV-1 DNA and (**c**) 2LTR circle DNA. Values are shown as means±standard errors

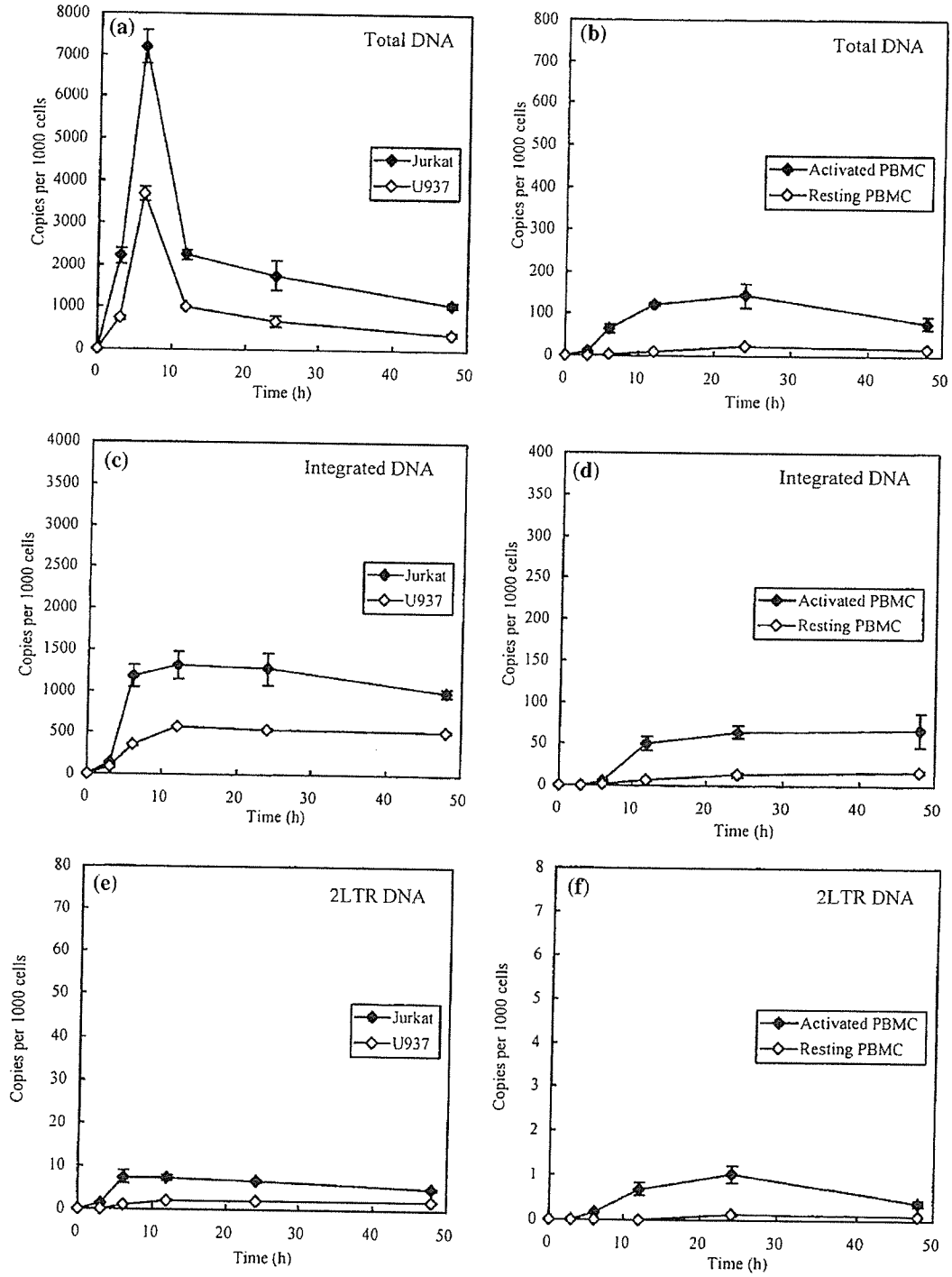

Fig. 4 Quantification of HIV-1 DNA synthesis during a single round infection of Jurkat cells, U937 cells, PHA/IL-2 activated PBMCs and resting PBMCs with VSV-G-pseudotyped NL-E delta env virus. (**a**) Time course analysis of total HIV-1 DNA synthesis in Jurkat cells and U937 cells, and (**b**) in PHA/IL-2 activated PBMCs and resting PBMCs. (**c**) Time course analysis of HIV-1 DNA integration in Jurkat cells and U937 cells, and (**d**) in PHA/IL-2 activated PBMCs and resting PBMCs. (**e**) Time course analysis of 2LTR DNA formation in Jurkat cells and U937 cells, and (**f**) in PHA/IL 2 activated PBMCs and resting PBMCs. Values are shown as means±standard errors

in the assay. The method 1 shown in Figs. 1 and 2 is equivalent to the real-time nested PCR developed by Brussel et al. and the method 2 is the new real-time nested PCR we have developed. Figs. 2a and b clearly demonstrated that specificity of our novel assay (method 2) was much higher than the previously reported method using a tag sequence. The probe-2 used in method 2 could inhibit the annealing of the residual tagged primer, which resulted in higher specificity than method 1.

By this novel assay, detailed kinetics of viral DNA synthesis was analyzed in Jurkat cells. Our assay detected integrated HIV-1 DNA within 3 h of infection, which emphasizes the sensitivity of this assay.

Then, we analyzed the kinetics of HIV-1 integration in U937 cells, activated PBMCs and resting PBMCs in addition to Jurkat cells. The kinetics of viral DNA integration depended on the cell type. HIV-1 DNA integration was completed 12 h after infection in Jurkat cells and U937 cells, 24 h in activated PBMCs and 48 h in resting PBMCs. Efficiency of viral integration was correlated with activity of reverse transcription. Jurkat cells exhibited the most rapid kinetics of reverse transcription and integration, and we may find the new factor(s) associated with reverse transcription and integration by investigating the molecules up-regulated or down-regulated in Jurkat cells.

The specific, sensitive and quantitative assay we have developed should prove useful in the kinetic studies of the integrated HIV-1 DNA especiallly during the early phase of infection. It should also prove applicable to clinical studies of viral integration and assessments of the effectiveness of future integrase inhibitors. Furthermore, it may be a valuable tool to test the integration efficiency of retroviral vectors designed for gene therapies.

Acknowledgements We thank Dr. Naoki Yamamoto for his support and helpful discussions. This work was supported by grants from the Ministry of Education, Science and Culture and the Ministry of Health, Labor and Welfare of Japan.

References

1. G. Englund, T.S. Theodore, E.O. Freed, A. Engleman, M.A. Martin, J. Virol. **69**, 3216–3219 (1995)
2. R.L. LaFemina, C.L. Schneider, H.L. Robbins, P.L. Callahan, K. LeGrow, E. Roth, W.A. Schleif, E.A. Emini, J. Virol. **66**, 7414–7419 (1992)
3. H. Sakai, M. Kawamura, J. Sakuragi, S. Sakuragi, R. Shibata, A. Ishimoto, N. Ono, S. Ueda, A. Adachi, J. Virol. **67**, 1169–1174 (1993)
4. M. Stevenson, T.L. Stanwick, M.P. Dempsey, C.A. Lamonica, EMBO J. **9**, 1551–1560 (1990)
5. M.I. Bukrinsky, N. Sharova, M.P. Dempsey, T.L. Stanwick, A.G. Bukrinskaya, S. Haggerty, M. Stevenson, Proc. Natl. Acad. Sci. USA **89**, 6580–6584 (1992)
6. M.I. Bukrinsky, N. Sharova, T.L. McDonald, T. Pushkarskaya, W.G. Tarpley, M. Stevenson, Proc. Natl. Acad. Sci. USA **90**, 6125–6129 (1993)
7. C.M. Farnet, F.D. Bushman, Cell **88**, 483–92 (1997)
8. L. Li, K. Yoder, M.S. Hansen, J. Olvera, M.D. Miller, F.D. Bushman, J. Virol. **74**, 10965–10974 (2000)
9. M.D. Miller, C.M. Farnet, F.D. Bushman, J. Virol. **71**, 5382–5390 (1997)
10. P. Barbosa, P. Charneau, N. Dumey, F. Clavel, AIDS Res. Hum. Retroviruses **10**, 53–59 (1994)
11. S.Y. Kim, R. Byrn, J. Groopman, D. Baltimore, J. Virol. **63**, 3708–3713 (1989)
12. T.W. Chun, L. Stuyver, S.B. Mizell, L.A. Ehler, J.A. Mican, M. Baseler, A.L. Lloyd, M.A. Nowak, A.S. Fauci, Proc. Natl. Acad. Sci. USA **94**, 13193–13197 (1997)
13. S. Sonza, A. Maerz, N. Deacon, J. Meanger, J. Mills, S. Crowe, J. Virol. **70**, 3863–3869 (1996)
14. R.J. Britten, W.F. Baron, D.B. Stout, E.H. Davidson, Proc. Natl. Acad. Sci. USA **85**, 4770–4774 (1988)
15. R. Kumar, N. Vandegraaff, L. Mundy, C.J. Burrell, P. Li, J. Virol. Methods **105**, 233–246 (2002)
16. N. Vandegraaff, R. Kumar, C.J. Burrell, P. Li, J. Virol. **75**, 11253–11260 (2001)
17. U. O'Doherty, W.J. Swiggard, D. Jeyakumar, D. McGain, M.H. Malim, J. Virol. **76**, 10942–10950 (2002)
18. A. Brussel, P. Sonigo, J. Virol. **77**, 10119–10124 (2003)
19. S.L. Butler, M.S. Hansen, F.D. Bushman, Natl. Med. **7**, 631–634 (2001)
20. S.L. Butler, E.P. Johnson, F.D. Bushman, J. Virol. **76**, 3739–3747 (2002)